RESEARCH ARTICLE | JULY 31 2024

Three-dimensional matrix stiffness modulates mechanosensitive and phenotypic alterations in oral squamous cell carcinoma spheroids

Special Collection: Physical Sciences Approaches to Cancer Research

Maulee Sheth ; Manju Sharma; Maria Lehn ; HasanAl Reza ; Takanori Takebe ; Vinita Takiar ; Trisha Wise-Draper ; Leyla Esfandiari

APL Bioeng. 8, 036106 (2024)
https://doi.org/10.1063/5.0210134

Three-dimensional matrix stiffness modulates mechanosensitive and phenotypic alterations in oral squamous cell carcinoma spheroids

Cite as: APL Bioeng. **8**, 036106 (2024); doi: 10.1063/5.0210134
Submitted: 25 March 2024 · Accepted: 22 July 2024 ·
Published Online: 31 July 2024

Maulee Sheth,[1] Manju Sharma,[1] Maria Lehn,[2] HasanAl Reza,[3] Takanori Takebe,[3,4] Vinita Takiar,[5,6] Trisha Wise-Draper,[2,6] and Leyla Esfandiari[1,6,7,8,a)]

AFFILIATIONS

[1]Department of Biomedical Engineering, University of Cincinnati, Cincinnati, Ohio 45221, USA
[2]Division of Hematology/Oncology, Department of Internal Medicine, University of Cincinnati College of Medicine, Cincinnati, Ohio 45219, USA
[3]Division of Gastroenterology, Hepatology and Nutrition and Division of Developmental Biology, and Center for Stem Cell and Organoid Medicine (CuSTOM), Cincinnati Children's Hospital Medical Center, Cincinnati, Ohio 45229, USA
[4]Department of Pediatrics, University of Cincinnati College of Medicine, Cincinnati, Ohio 45229, USA
[5]Department of Radiation Oncology, University of Cincinnati College of Medicine, Cincinnati, Ohio 45219, USA
[6]University of Cincinnati Cancer Center, Cincinnati, Ohio 45267, USA
[7]Department of Electrical Engineering and Computer Science, University of Cincinnati, Cincinnati, Ohio 45221, USA
[8]Department of Environmental and Public Health Sciences, University of Cincinnati, Cincinnati, Ohio 45267, USA

Note: This paper is part of the special issue on Physical Sciences Approaches to Cancer Research.
[a)]**Author to whom correspondence should be addressed:** esfandla@ucmail.uc.edu

ABSTRACT

Extracellular biophysical cues such as matrix stiffness are key stimuli tuning cell fate and affecting tumor progression *in vivo*. However, it remains unclear how cancer spheroids in a 3D microenvironment perceive matrix mechanical stiffness stimuli and translate them into intracellular signals driving progression. Mechanosensitive Piezo1 and TRPV4 ion channels, upregulated in many malignancies, are major transducers of such physical stimuli into biochemical responses. Most mechanotransduction studies probing the reception of changing stiffness cues by cells are, however, still limited to 2D culture systems or cell-extracellular matrix models, which lack the major cell–cell interactions prevalent in 3D cancer tumors. Here, we engineered a 3D spheroid culture environment with varying mechanobiological properties to study the effect of static matrix stiffness stimuli on mechanosensitive and malignant phenotypes in oral squamous cell carcinoma spheroids. We find that spheroid growth is enhanced when cultured in stiff extracellular matrix. We show that the protein expression of mechanoreceptor Piezo1 and stemness marker CD44 is upregulated in stiff matrix. We also report the upregulation of a selection of genes with associations to mechanoreception, ion channel transport, extracellular matrix organization, and tumorigenic phenotypes in stiff matrix spheroids. Together, our results indicate that cancer cells in 3D spheroids utilize mechanosensitive ion channels Piezo1 and TRPV4 as means to sense changes in static extracellular matrix stiffness, and that stiffness drives pro-tumorigenic phenotypes in oral squamous cell carcinoma.

INTRODUCTION

Biophysical alterations in the tumor microenvironment are one set of key components disrupting tissue homeostasis and driving cancer. These alterations can be attributed to four distinct mechanical hallmarks of cancer, namely, elevated solid stress, increased interstitial fluid pressure, augmented stiffness, and altered tissue microarchitecture known to further regulate cell fate.[1,2] In particular, increased extracellular matrix (ECM) stiffness is a mechanical characteristic of solid tumors that has been shown to regulate and promote biological hallmarks of cancer, including growth, metabolism, invasion, and metastasis in several cancer types.[3,4] Much of the seminal work revealing the regulation of cell function by matrix stiffness was enabled by the pioneering development of a

polyacrylamide-based cell culture system with tunable elastic modulus by Pelham and Wang.[5] This system enabled some of the first studies investigating the effect of matrix stiffness on cancer cell function.[6] The utility of 2D culture systems such as this one is, however, limiting since the complex 3D structural and topographical features of tumors are not recapitulated. The advent of 3D culture techniques such as spheroids and tumor-on-chip platforms has bridged this gap and revolutionized *in vitro* preclinical models capable of better mimicking the genetic, proteomic, morphological, and pharmacological features of tumors *in vivo*.[7]

Over the past few years, studies adopting 3D culture systems to look at the influence of matrix stiffness on cancer spheroid behavior have emerged. In breast cancer, matrix stiffness has been reported to regulate the growth of breast cancer tumor spheroids and their response to chemotherapy using collagen-alginate hydrogels of varying stiffness.[8] Another set of studies investigated that matrix stiffness-mediated mechanotransduction regulated 3D spheroid sorting and collective migration, cell viability, morphology, and invasion as well as EMT and tumor metastasis using spheroids generated from breast cancer cell lines.[9–11] In ovarian cancer, mechanical stiffness of the underlying fibronectin-coated hydrogel substrate has been found to directly regulate spheroid disaggregation, indicative of the effect of ECM stiffening on spheroid invasion *in vivo*.[12] Using a PEGDA-printed tumor-on-a-chip platform, Amereh *et al.* investigated the influence of matrix stiffness on the growth and invasion of human glioblastoma tumoroids.[13] Importantly, the influence of matrix stiffness on cell behavior is also highly dependent on the cell type and the biomaterial being used. As such, the responses of cancer spheroids to the mechanical environment are being increasingly well characterized, but the specific modalities by which cells in 3D spheroids, particularly in oral squamous cell carcinoma, sense differences in ECM stiffness remain to be probed.

Cancer cells are equipped with a variety of mechanosensory components, including integrins, cadherins, and mechanosensitive cation channels (MSCs) that sense changes in mechanical cues and transduce them into biochemical signaling pathways fostering malignant cell behavior. Piezo channels and some transient receptor potentials (TRPs) are the two most distinctive MSC families involved in cancer. Mechanosensitive Piezo1 ion channels, upregulated in many malignancies, mostly of epithelial origin are polymodal sensors of diverse mechanical forces, including osmotic pressure, fluid shear stress, substrate stiffness, and confinement.[14,15] Among the TRP superfamily of ion channels, TRPV4 (vanilloid receptor family member IV) is a non-selective MSC involved in different types of cancer, activated by cell swelling, shear stress, moderate temperatures, hypoosmotic conditions, and chemical agonists.[16,17] Additionally, TRPV4 also acts as a sensor of ECM stiffness.[18] Overexpression of Piezo1 and TRPV4 intervenes in cancer progression by influencing several tumor-related mechanisms, including proliferation, apoptosis, angiogenesis, migration, and invasion.[14,19–21] Most stiffness-activated Piezo1 and TRPV4 mechanotransduction studies are, however, still limited to dynamic environments or two-dimensional culture models.[22–24] Additionally, these studies are largely restricted to assessing the influence of matrix stiffness on single cells and thereby lack prominent cell–cell interactions in tumors. To this end, whether and how cancer spheroids in a 3D microenvironment utilize MSCs such as TRPV4 or Piezo1 ion channels to sense matrix stiffness cues remains to be seen.

Head and neck squamous cell carcinoma (HNSCC) is the seventh most common cancer globally.[25] Mechanopathology of oral squamous cell carcinoma (OSCC), an HNSCC malignancy, has been reported to have a 3.6-fold increase in tissue stiffness as compared to normal counterpart tissue owing to ECM remodeling.[26] Overall, a stiffened matrix has been correlated with poor survival and post-surgical recurrence in OSCC.[27,28] However, biophysical mechanisms by which stiffening of the ECM drives OSCC progression remain to be determined. Here, we engineered a 3D spheroid culture environment with varying biomechanical properties to study the effect of static matrix stiffness stimuli on mechanosensitive and tumorigenic components in OSCC tumors. Cal27 spheroids cultured in varying stiffnesses were monitored for growth and assessed for Piezo1 and stemness marker CD44 protein expressions. Matrix stiffness was found to have a profound influence on the transcriptomic level of Cal27 spheroids with specific selections of genes involved in mechanoreception, ECM organization, ion channel transport, and pro-tumorigenic phenotypes found to be upregulated in spheroids cultured in the stiff ECM. Taken together, the results suggested that cancer spheroids respond to static matrix stiffness cues through mechanosensory Piezo1 and TRPV4 ion channels, and that stiffness drives phenotypic alterations driving cancer progression in OSCC spheroids. Overall, our proof-of-concept study demonstrated that the extension and utility of this model, with future incorporation of multiple cell types and patient-derived cells, have immense potential to serve as a relevant *in vitro* system to study the effect of targeting ECM stiffness and mechanosensors as emerging strategies to treat cancer.[19]

RESULTS

Mechanical characterization of soft and stiff hydrogels

Healthy marginal tissue from squamous cell hyperplasia has been reported to have Young's modulus of 0.9 ± 1.2 kPa using Atomic Force Microscopy (AFM). This is significantly softer than 4 ± 5.5 kPa for squamous cell carcinoma tissue.[26] In our study, Growth Factor Reduced (GFR) Matrigel at 3 and 12 mg/ml concentrations was used to simulate a soft and stiff ECM, respectively, for 3D cell culture conditions [Fig. 1(a)]. Since the length scale of the testing method factors into elastic modulus measurements, hydrogels were characterized two-fold at different measurement scales—macroscale using rheometry and microscale using AFM.[29] Rheological strain sweep of 20 mm hydrogel samples indicated an increase in the loss (G'') and storage (G') moduli with concentration with a linear viscoelastic response observed up to 50% strain [Figs. 1(b) and 1(c)]. Mechanical characterization by shear rheology indicated an eightfold increase in storage (G') and Young's (E) moduli at the bulk level with the storage modulus being 0.0096 ± 0.0006 kPa for soft and 0.0828 ± 0.0130 kPa for stiff conditions [Fig. 1(d)]. Mean stiffness (E) was found to be $0.028\,93 \pm 0.0018$ and 0.2485 ± 0.0390 kPa for soft and stiff conditions, respectively [Fig. 1(d)]. Since local inhomogeneity in stiffness can occur, a total of hundred subsequent locations were measured using AFM for each sample (supplementary material Fig. S1). AFM indicated a threefold increase in stiffness at the intermolecular level with mean Young's moduli (E) being 0.3183 ± 0.1547 and 0.8898 ± 0.1109 kPa for soft and stiff hydrogels, respectively [Fig. 1(e)].

Spheroid size positively correlates with matrix stiffness over time in culture

Spheroids grown in soft and stiff conditions were assessed for growth and morphology over a culture period of 14 days. Day 14 spheroids were visualized using immunofluorescent staining for the nuclei

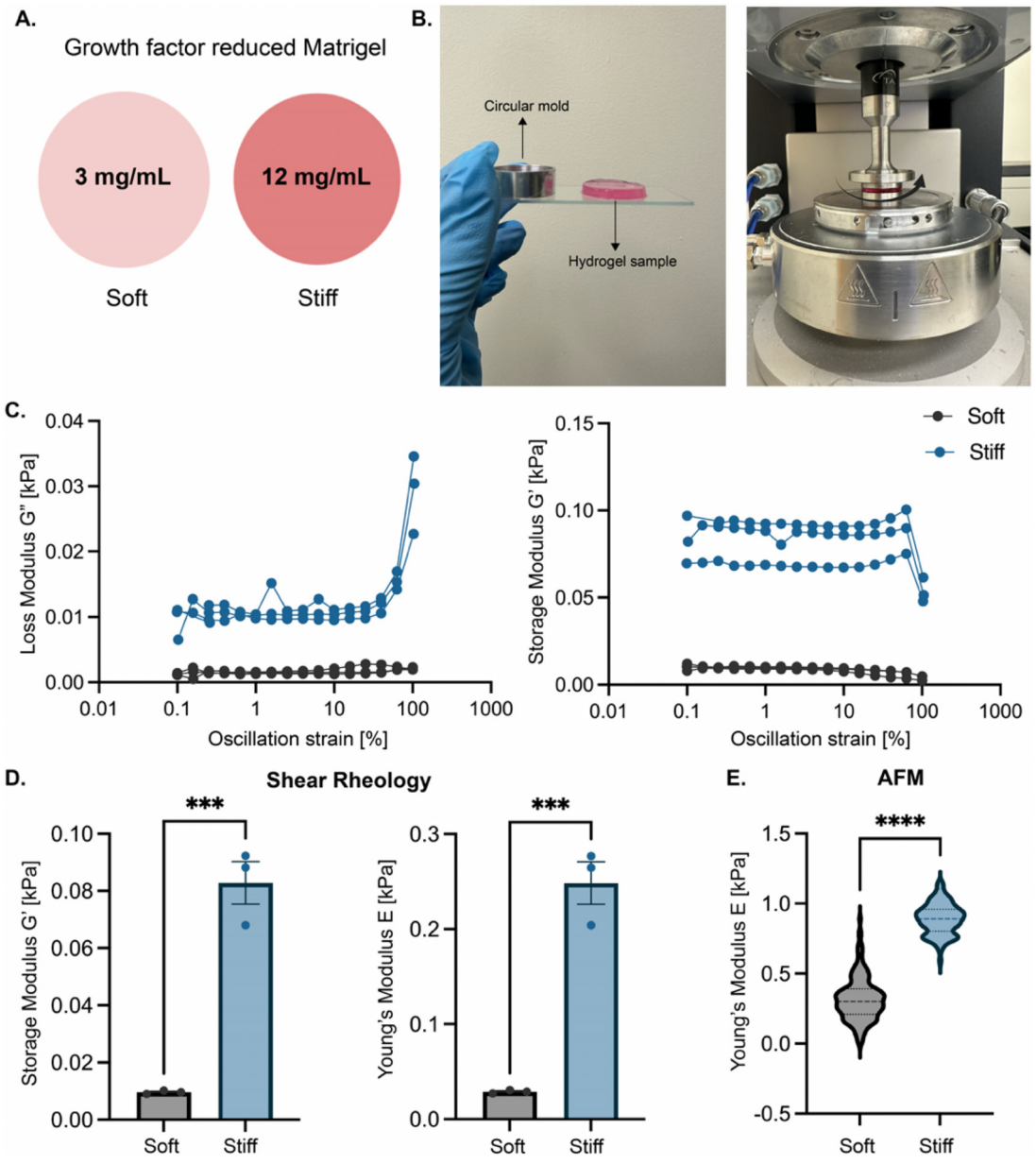

FIG. 1. Mechanical characterization of (a) soft and stiff Matrigel defined by 3 and 12 mg/ml concentrations, respectively. (b) 20 mm circular hydrogel samples were fabricated using a mold for mechanical testing (left). Shear rheology testing setup with a loaded sample (right) (c). Oscillation strain curves indicating loss (G″) and storage (G′) moduli for soft and stiff hydrogels, respectively. Measurements are taken over an oscillation strain range from 0.1% to 100% (n = 3 each) (d). Relative storage (G′) and Young's (E) moduli derived at 1% strain from shear rheology (n = 3 each) (e). Relative Young's (E) moduli measured by atomic force microscopy (n = 3 each). Data are represented as mean ± SEM. $^{***}p < 0.001$ and $^{****}p < 0.0001$.

(DAPI), and Piezo1 (FITC) and CD44 (APC) target markers using confocal microscopy with z-stacks performed across the spheroid height [Figs. 2(a) and 2(b)]. Spheroid growth assessment over time in culture indicated increased surface area for samples under stiff conditions as compared to those in soft conditions. This increase in area was observed to be more prominent beyond six days of culture [Fig. 2(c)]. Quantitative analysis of day 14 spheroids indicated a significant increase in average diameter [Fig. 2(d)] and surface area [Fig. 2(e)] with increase in stiffness, while no significant difference was observed in the average number of cells per spheroid between the two groups (supplementary material Figs. S2 and S3). Soft matrix spheroids were found to have an average diameter of 135.8 ± 19.9 μm. This value increased to 243.0 ± 46.2 μm for stiff

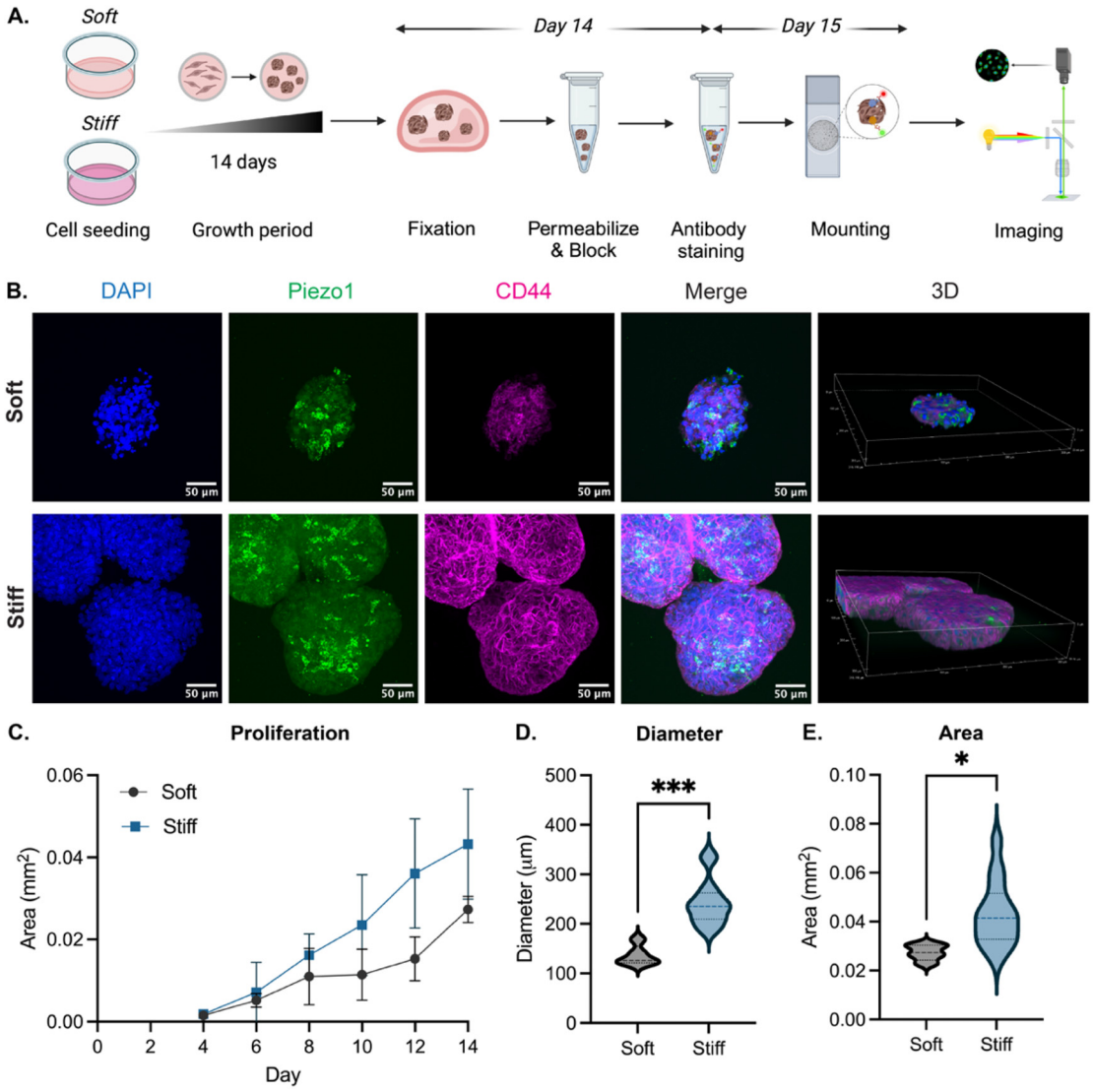

FIG. 2. Morphological analysis of Cal27 spheroids grown in soft and stiff matrix conditions (a). Workflow indicating experimental timeline and procedure breakdown (b). Representative confocal z-stack maximum intensity and 3D alpha blended projections of day 14 spheroids cultured in soft and stiff conditions, stained for the nuclei (DAPI), Piezo1 (green), and CD44 (magenta). Scale bar = 50 μm. (c). Temporal evolution of tumor area over 14 days in culture for both conditions. Each solid mark represents the average of at least n = 15 spheroids with SEM. (d) Relative diameter and (e). Surface area of day 14 spheroids. $^{*}p < 0.05$ and $^{***}p < 0.001$.

matrix spheroids. Average spheroid area was found to be 0.027 ± 0.003 and 0.043 ± 0.013 mm^2 for soft and stiff conditions, respectively.

3D matrix stiffness regulates Piezo1 activity and stemness marker expression

To study the role of matrix stiffness on Piezo1 expression, spheroids grown in soft and stiff conditions were harvested and lysed into single cells upon 14 days of culture for flow cytometry analysis [Fig. 3(a)]. Figure 3(b) shows relevant controls including unstained and isotype samples. Flow cytometric analysis indicated a 2.8-fold increase in mean Piezo1 expression with $12.9\% \pm 4.0\%$ positive cells for stiff conditions as compared to $4.6\% \pm 3.7\%$ positive cells for soft conditions [Figs. 3(c) and 3(d)]. A similar positive trend was observed for the CD44 cancer stem cell-like marker with a 1.2-fold increase in mean expression with $87.0\% \pm 8.0\%$ positive cells for stiff conditions as compared to $73.5\% \pm 10.3\%$ positive cells for soft conditions [Figs. 3(e) and 3(f)]. Immunofluorescence imaging of frozen spheroid sections indicated that the presence of Piezo1 and CD44 is relatively uniform across soft matrix-derived spheroids and appears to become more prominent toward the peripheral regions for stiff matrix spheroids (supplementary material Fig. S4). Taken together, this suggests that Piezo1 is a mechanosensor of static matrix stiffness, and that OSCC progression is regulated in a 3D matrix stiffness-dependent manner.

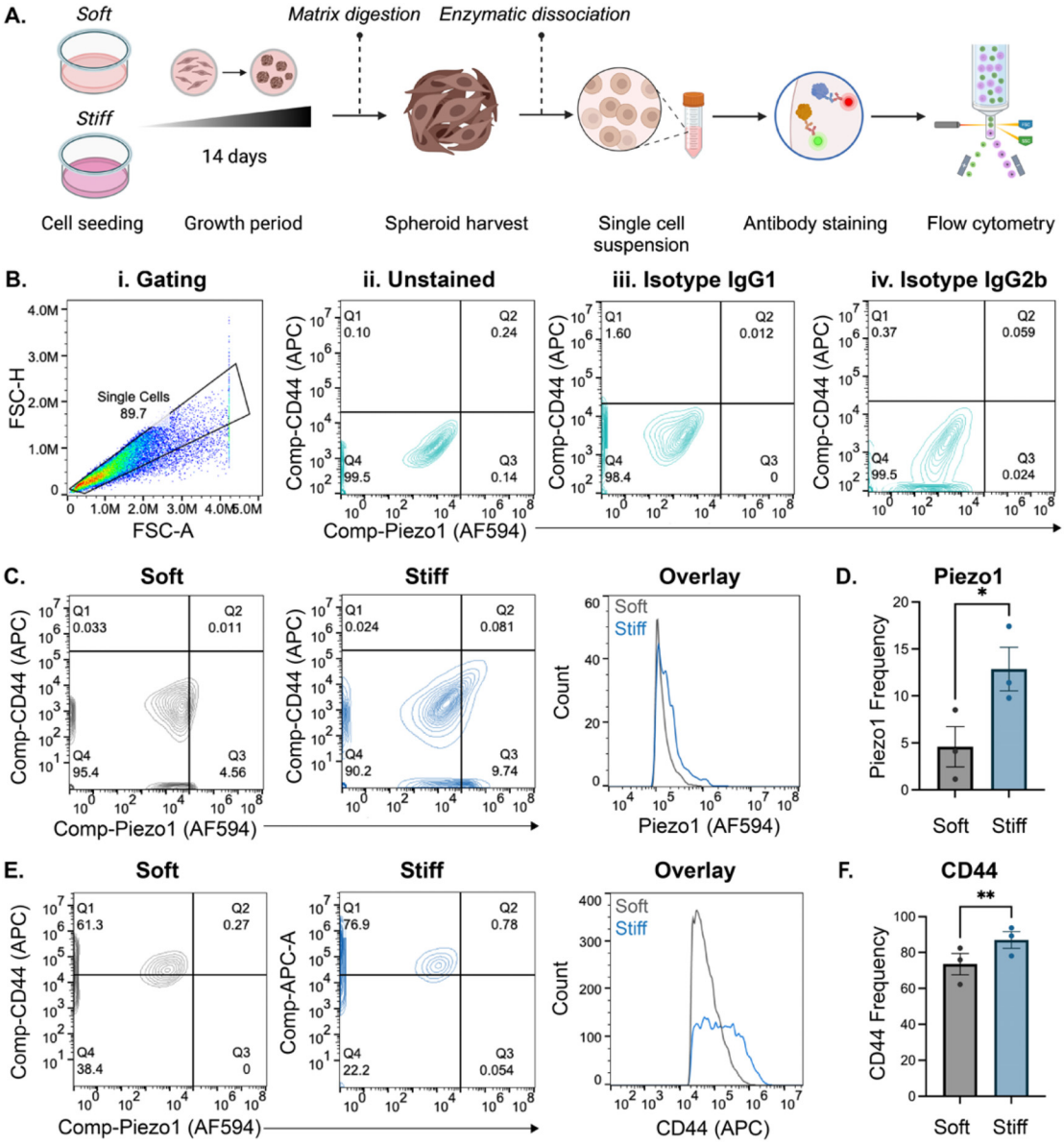

FIG. 3. 3D matrix stiffness regulates Piezo1 and CD44 expressions in Cal27 spheroids post 14 days of culture. (a) Workflow indicating experimental timeline and procedure breakdown. (b) Flow cytometry controls indicating (i) gating of single cells and (ii) unstained and isotype controls for (iii) IgG1 and (iv) IgG2b. (c). Representative contour plots and histogram indicating relative Piezo1 expression between soft and stiff conditions (d). Quantitative analysis of Piezo1 positivity marked by percentage of positive cells ($n = 3$ each) (e). Representative contour plots and histogram indicating relative CD44 expression between soft and stiff conditions (f). Quantitative analysis of CD44 positivity marked by percentage cells ($n = 3$ each). Data are represented as mean ± SEM. $^{*}p < 0.05$ and $^{**}p < 0.01$.

Matrix stiffness influences a broad set of transcripts in Cal27 spheroids

To study the role of matrix stiffness at a transcriptomic level, spheroids grown in soft and stiff conditions were harvested upon 14 days of culture, and total RNA isolation and sequencing was performed [Fig. 4(a)]. Quality control of samples ($n = 3$ per condition) revealed good concentration and integrity of RNA (supplementary material Table S1). Visualization of the likeness between transcriptomic profiles of samples using principal component analysis (PCA) indicated a 97% variance in the mRNA composition of spheroids grown in soft and stiff conditions, with high consistency across biological replicates, upon 14 days of culture [Fig. 4(b)]. Substrate stiffness elicited a pronounced impact on the transcriptome with 4778 DEGs (log2FoldChange $> |0.58|$ and q-value $<= 0.05$) between the soft and stiff matrix groups [Fig. 4(c)]. Of these, 2581 genes were upregulated (negative log2FoldChange), while 2197 genes were downregulated (positive

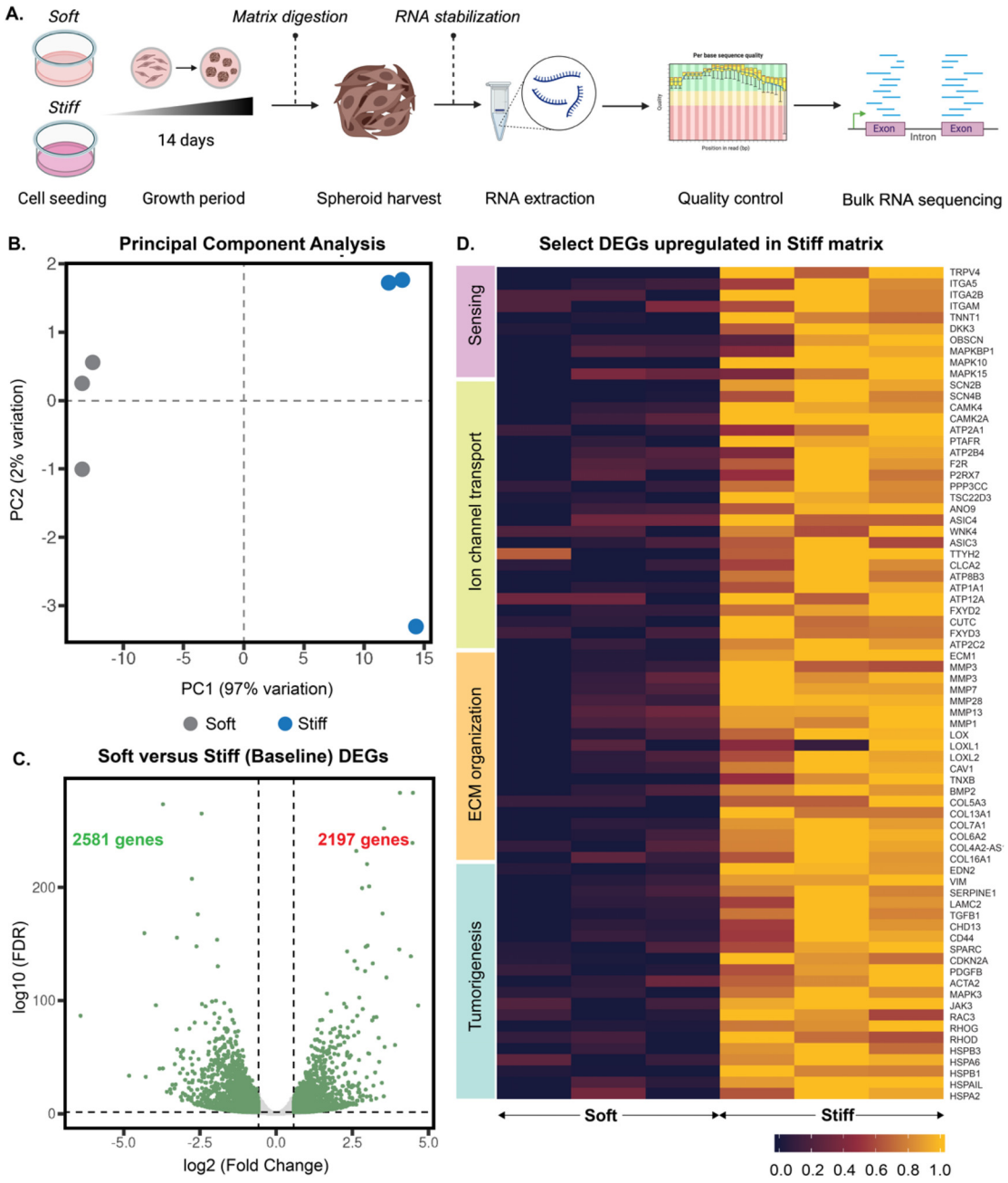

FIG. 4. Matrix stiffness alters gene expression profiles of Cal27 spheroids after 14 days of culture (a). Workflow indicating experimental timeline and procedure breakdown (b). Principal component analysis wherein PC1 explains 97% of the variance and PC2 explains 2% of the variance. Gray dots indicate soft matrix samples (n = 3), and blue dots indicate stiff matrix samples (n = 3) (c). Volcano plot (log2fold change vs log10FDR) of stiffness-dependent differentially expressed genes (DEGs) (log2FoldChange $>$ |0.58| and q-value $<=$ 0.05). Negative fold change indicates relatively increased expression in spheroids in stiff matrices (green font), and positive fold change indicates relatively decreased expression in spheroids in stiff matrices (red font) quantified by RNA sequencing (d). Heatmap of a selection of DEGs upregulated in stiff matrix samples with yellow indicating relatively high expression and violet indicating relatively low expression of genes specified row-wise for samples specified column-wise (n = 3 per group).

log2FoldChange) in stiff matrices [Fig. 4(c)]. A heatmap of all DEGs across the two groups is provided in the supplementary material (supplementary material Fig. S5). To assess the influence of increased matrix stiffness on mechanosensitive and malignant phenotypes in OSCC spheroids, we looked at a selection of upregulated DEGs with associations to mechanotransduction [Fig. 4(d), boxed in lilac], ECM organization [Fig. 4(d), boxed in orange], ion channel transport [Fig. 4(d), boxed in green], and tumorigenesis [Fig. 4(d), boxed in blue].

Critical mechano-signal transducers are overexpressed in stiff matrix spheroids

It has been well established that both the ECM itself and ECM stiffening-induced mechanical stimuli may activate cell membrane receptors and mechanosensors such as integrin, Piezo1, and TRPV4, thereby modulating the malignant phenotype of tumor cells.[19] RNA sequencing performed in this study revealed that the TRPV4 nonselective cation channel was significantly overexpressed in the stiff substrate groups. TRPV4 is a critical sensor of matrix stiffness cues and is implicated in regulating cancer cell motility, invasion, and extravasation. Additionally, TRPV4 can also promote matrix stiffness-induced EMT.[20,30] Interestingly, the Piezo1 gene was not found to be significantly differentially expressed between the soft and stiff matrix conditions. Several genes reported to have associations with Piezo1 activity including DKK3, OBSCN, TNNT1, MAPK-10, -15, and -BP1 were, however, found to be upregulated in the stiff matrix groups.[31] As mentioned previously, integrin is another critical transducer that mediates the tumor-promoting effects of ECM stiffening in cancer.[19] In line with this, our sequencing results revealed overexpression of certain members of the integrin subunit alpha family including ITGA5, ITGA2B, and ITGAM in spheroids cultured in stiff matrices.

Mechanical stiffness influences ion transport in a mechanoelectrical coupling manner

Interestingly, sodium voltage-gated channel beta subunits SCN2B and SCN4B were two of the five maximally upregulated genes in the stiff matrix groups. Sodium channel gating kinetics of these genes are involved in cell action potential along with cell–cell adhesion and cell migration.[32] Furthermore, a set of genes associated with ion channel transport including ATP-8B3, -2A1, -12A, -1A1, CLCA2, ASIC3, ASIC4, WNK4, FXYD2, and CUTC were found to be upregulated in stiff matrix spheroids.[33–36] Genes with involvement in calcium signaling such as PRKCA, F2R, CAMK4, and CAMK2A were also observed to be upregulated in the stiff matrix groups.[37,38] This differential expression of genes involved in ion channel transport, particularly those without a primarily mechanosensitive modality, indicates the potential influence of 3D matrix stiffness on cellular depolarization in squamous cell carcinoma spheroids.

Extracellular matrix stiffness regulators are upregulated in stiff matrices

ECM regulators such as COL5A3, ECM1, TNXB, COL13A1, SERPINE1, TGFB1, and BMP2 were all upregulated on stiff matrices as compared to the soft ones.[39] Additionally, lysyl oxidase (LOX) family genes, including LOX, LOXL1, and LOXL2, and matrix metalloproteinases (MMPs), including MMP1, MMP7, and MMP9, were also upregulated in spheroids cultured in stiff substrates. The LOX family proteins are major molecules contributing to matrix cross-linking, which is critical for stiffening cancer tissue.[40] Additionally, broader microenvironmental changes triggered by LOX family oxidases, in synergy with stiff ECM, promote cancer cell proliferation and invasion.[41] Similarly, the MMP family of zinc-dependent proteinases plays a crucial role in ECM maintenance and remodeling by degrading ECM proteins and playing a role in several stages of the multistep carcinogenesis cascade.[40] Caveolin-1 (CAV1) was another ECM-regulating gene found to be upregulated in the stiff matrix groups. CAV1 controls focal adhesion stability, actin reorganization, and actomyosin contraction and participates in mechanotransduction driving ECM remodeling.[42] Overall, these results indicate the presence of a feedback loop mechanism wherein stiff substrates stimulate the expression of ECM-regulating genes associated with matrix remodeling, giving rise to increasingly stiff and tumorigenic ECM.

Stiff matrix spheroids exhibit enhanced tumorigenic and malignant phenotypes

Endothelin-2 (EDN2) and Vimentin (VIM) were another two of the ten maximally upregulated genes in stiff matrix spheroids. Both these genes are associated with malignant progression with EDN2 involved in tumorigenesis and VIM playing a role in cell attachment, migration, and metastasis.[20] Certain other genes such as MAPK3, RAC3, JAK3, and Rho-GTPases RHOG and RHOD with associations to cancer-promoting signals were also found to be upregulated in stiff hydrogel spheroids.[43,44] Stiff substrate groups also indicated the presence of common EMT-associated genes in cancer such as CD44, COL5A3, SERPINE1, LAMC2, TGFB1, CDH13, SPARC, and certain integrins.[45,46] Additionally, genes associated specifically with tumor progression in OSCC including CDKN2A and PDGFB were also found to be upregulated with stiffness.[47] Interestingly, certain members of the heat shock protein (Hsp)-associated genes including HSPB3, HSPA6, HSPB1, HSPA1L, and HSPA2 that play a key role in regulating cancer cell tumorigenicity in response to mechanical stresses were another set of genes upregulated in stiff groups.[48] These findings indicate that elevated matrix stiffness induces a malignant phenotype in squamous cell carcinoma spheroids.

DISCUSSION

Our study aims to explore how matrix stiffness influences cell behavior in three-dimensional spheroids as a static biomechanical cue. Mechanisms by which spheroids sense differences in ECM stiffness can be highly dependent on both—the cells utilized to form the spheroids and the biomaterial used to mimic the ECM. Here, we utilized a Matrigel-based liquid overlay platform for three-dimensional culture of Cal27 oral squamous cell carcinoma spheroids. The formation of Matrigel consisting of ECM-rich proteins including laminin, collagen IV, and entactin enables effective culturing of 3D spheroids and organoids and has been widely utilized in cancer research.[49] Matrigel has also been found to have a more homogenous network structure as compared to other ECM protein-based hydrogels.[50] In our study, the utility of growth factor reduced (GFR) Matrigel resulted in a reduction of abundance levels of growth factors minimizing their influence on cell behavior between groups.[51] Batch-to-batch variability, another challenge associated with Matrigel, was mitigated by utilizing the same batch of products for replicate experiments throughout the study. However, it is important to note that since stiffness was controlled by varying Matrigel concentration, other overarching factors could also be influencing spheroid growth between the two groups. As such, since hydrogel stiffness is generally controlled by varying polymer concentrations, the resulting change in pore size (and thus in transport properties) and a varying density of cell adhesion sites could also affect spheroid growth.[52] For instance, gel stiffness, cell migration speed, and particle diffusion have been reported to correlate with a certain degree, which is largely attributed to differences in gel microarchitecture.[53] In

general, increased protein concentration results in smaller pore sizes and higher gel stiffness (Matrigel has been reported to have a pore size of ∼0.30 nm at a concentration of 3.5 mg/ml and ∼0.14 nm at 7.4 mg/ml).[50,53] It is worthwhile to note that Zaman *et al.* have previously reported that since Matrigel pore sizes are much smaller than cellular dimensions (as opposed to hydrogels such as collagen), pore size exerts less of an influence on migration as compared to mechanical stiffness, cell-matrix adhesion, and proteolysis.[54] Decoupling the role of matrix stiffness and biochemical properties while utilizing more native ECM-like hydrogels, however, remains a prevailing challenge in probing spheroidal colony growth under varying stiffness stimuli.[52]

Mechanical characterization of hydrogels revealed an 8- and threefold increase in matrix stiffness from soft to stiff groups using shear rheology and AFM, respectively. AFM indicated a stiffness of ∼0.3 kPa for our soft and ∼1 kPa for our stiff hydrogels, reflective of the lower pathologic stiffness range of 0.9 ± 1.2 kPa for marginal healthy tissue and 4 ± 5.5 kPa for squamous cell carcinoma tissues.[26] AFM indentations indicated certain heterogeneity in measurements between subsequent locations. Whether the nonuniform points are due to a dead zone, consecutive indentations, temperature change, or due to spatial technical issues is uncertain. Such local inhomogeneity in the mechanical properties of ECMs and tissues has been heavily reported with multiple-point measurements commonly used to mitigate the influence of outliers.[26] Additionally, while bulk rheometry is a macroscopic test method that exposes testing samples to oscillatory shear strains, AFM indentations probe highly localized surface properties of a material. Discrepancies between Young's modulus from rheological and AFM measurements for our samples are, thus, expected to have resulted from factors including length scale differences in test modes (bulk vs local), different stress modes (shear vs compression), and temperature conditions as reported previously.[55] The stiffness range achieved in this study while representative of the lower pathological elastic moduli of healthy and cancerous oral tissue is still low and cannot represent increasingly stiff tissues in advanced stages. Hydrogels facilitating spheroid culture as efficiently as Matrigel while also providing a larger range of tunability are worth investigating for this reason. However, it is also important to note that different hydrogels with the same stiffness can evoke different cellular responses owing to the presence of varying matrix proteins.[11]

Morphological analysis of spheroids cultured in soft and stiff Matrigel matrices showed that Cal27 cancer cells in stiff hydrogels developed into larger spheroidal colonies than those in the soft gels with a 58% increase in the average area. Such a positive correlation between ECM rigidity and cell spreading and morphology has been extensively studied.[3,8,12,56] Wong *et al.* have also shown that cancer cells exhibit robust growth of spheroids in stiff hydrogels that exert substantial confining stress on the cells.[48] This change in spheroid growth can be further attributed to the presence of a relationship between tumor stiffness and solid stress as described by Kalli and Stylianopoulos using the simple analogy of a spring that obeys Hooke's law. According to this theory, when a tumor grows and pushes the surrounding tissue, the total solid stress transmitted in the tumor interior is a combination of the external stress from the tissue and the growth-induced stress generated from mechanical interactions within the tumor. In the case that the tumor stiffens over time ($E_{tumor} > E_{tissue}$), it can push against the tissue and increase in size.[57] RNA sequencing performed in our study did show increased expression of collagen and LOX-family genes in spheroids in stiff ECM, indicating that the increase in size of spheroids in the stiff matrix can potentially be attributed to such matrix-induced stiffening of the spheroids. Additionally, we utilized immunofluorescence staining followed by confocal microscopy to visualize Piezo1 and CD44 in day 14 spheroids. However, considering challenges such as uneven antibody penetration through intact 3D structures of this size scale and differences in size between the two groups, confocal data were not utilized to quantify or localize marker expression. Protein marker analysis using flow cytometry indicated an increase in Piezo1 and CD44 expression levels with an increase in stiffness. Since bulk-level flow cytometry analyzes thousands of cells to quantify average expression levels and does not allow for probing of the origin of the cells analyzed, this was complemented by immunofluorescence staining of frozen spheroid sections. Imaging of sections indicated that Piezo1 expression is uniform over the spheroid section for soft matrix spheroids. This presence appears to be stronger toward peripheral regions for spheroids from the stiff matrices, potentially due to increased cell–ECM interactions and matrix mechanical forces.

A myriad of mechanisms and molecules are involved in the process of mechanosensation and tumor progression.[58] Mechanosensitive ion channels are pivotal players in these processes due to their capability of serving as excellent first responders, signal integrators, information encoders, and drug targets. As mentioned previously, matrix stiffness-induced mechanical stimuli primarily activate mechanoreceptors such as Piezo1 and TRPV4 ion channels and integrin.[19,30] In our study, mRNA levels for TRPV4 and certain integrins were found to be upregulated in stiff matrix spheroids indicating their role in sensing changes in stiffness cues. Since increased protein concentration has also been reported to express increased integrins for cell adhesion, decoupling the influence of stiffness on the integrins upregulated in our dataset needs to be further investigated.[54] Additionally, spheroids in the stiff ECM had higher levels of Piezo1 protein expression providing evidence that cancer cells in three-dimensional colonies can sense static mechanical stimuli by means of Piezo1 activity. Interestingly, the Piezo1 mRNA was not found to be differentially expressed between spheroids in the soft and stiff ECM. This non-significant Piezo1 mRNA change induced by matrix stiffness in our study contrasts with other studies, showing ECM stiffness-dependent regulation of Piezo1 mRNA levels.[24,59] However, it is worthwhile to note that these studies have been limited to cells in 2D environments or single cells in 3D, wherein cells are subjected to similar spatial dynamics. Conversely, cells in 3D spheroids are subjected to varying cell-cell and cell-ECM interactions depending on the spatial presence of the cells within a given spheroid. This comes with a potential possible loss of certain cell-specific genes when employing bulk RNA-sequencing. Furthermore, genome-wide correlation studies between expression levels of mRNA and protein are quite poor, hovering around 40% explanatory power with the discrepancy typically attributed to other levels of regulation between a transcript and a protein product.[60] In line with this, it has also been established that transcript levels are insufficient to predict protein levels in many biological scenarios, especially when cells are adjusting to changes in environmental conditions.[61] Additionally, it has been shown that some cancer cells can alter phenotype without significant changes to the transcriptome.[62] Whether the lag between the Piezo1 protein and mRNA levels in our study is driven by spatial or timescale factors or post-translational mechanisms remains to be investigated.

We have previously reviewed the role of dysregulation of the bioelectric state of cancer cells affecting all three processes of carcinogenesis, including initiation, promotion, and progression.[63] The upregulation of multiple genes involved with ion channel transport especially those with primary voltage sensing modalities, such as SCN2B and SCN4B, in our stiff matrix spheroids, provides preliminary evidence of the presence of mechano-electric crosstalk wherein biomechanical cues from the ECM influence the membrane potential (V_{mem}) of cancer cells. Such a relationship between V_{mem} and the mechanical properties of the microenvironment was first reported by Silver *et al.* wherein substrate stiffness was found to tune V_{mem} in mammary epithelial cells.[64] Indeed, V_{mem} has been known to function at the interface of chemical and mechanical signals by creating an electrical gradient across cells, which, in turn, gates voltage-sensitive channels to create a tightly communicated pathway between a cell and its microenvironment.[63,65]

In line with the biological relevance of stiff tissues being increasingly tumorigenic, several genes associated with progression and EMT were also upregulated in stiff matrix spheroids in our study. Both CD44 protein and mRNA levels were found to be upregulated in spheroids in stiff ECM. In tumor tissues, CD44 levels have been correlated with tumorigenesis in cancers including head and neck squamous cell carcinoma patients.[66] Stress-inducible Hsps, which are known to play a role in regulating cancer cell malignancy under mechanically stressed conditions, were another set of genes upregulated in our stiff matrix spheroids. Evidently so, in the same study mentioned previously, Wong *et al.* also found that the increased stressed condition in stiff hydrogel groups activated Hsps to mediate the survival of cancer cells, thereby upregulating the expression of stemness-related markers in colorectal cancer spheroids via TRPV4.[48] Finally, spheroids from the stiff matrix were also observed to have an upregulation of a set of genes involved in ECM remodeling. While this agrees with previous reports on matrix stiffness-induced cellular responses leading to increasingly stiffer matrices, it needs to be further probed, ideally with the incorporation of key cell types involved in ECM reorganization. Overall, our results demonstrate that varying matrix mechanical stiffness in a spheroid culture platform enhances spheroid growth and malignant phenotypes by employing Piezo1 and TRPV4 mechanoreceptors, suggesting that physical and biochemical cues exhibit dynamic interplay in OSCC. While our model is simplistic owing to the use of a single cell line, it provides evidence of the utility of mechanosensitive ion channels in sensing changes in ECM stiffness in 3D cancer spheroids. It is also important to note that while the utility of 3D culture techniques, including the one presented in this study, has enabled better mimicking of tumors *in vivo*, they do not replicate certain aspects such as the structural and mechanical heterogeneity found in real tumors. To this end, such platforms are a step closer to recapitulating *in vivo* tumors compared to two-dimensional platforms but need to be further developed to replicate such facets of real tumors.

CONCLUSIONS

Over the years, mechanobiology in cancer and how cells sense and respond to biophysical cues from the surrounding environment have been extensively probed. The role and utility of mechanical cues including ECM stiffness in cancer diagnosis, prognosis, and therapy has led to the relatively recent coining of terms such as "mechanopathology" and "mechanomedicine." We revealed that Piezo1 and TRPV4 receptors are involved in sensing changes in matrix stiffness in OSCC spheroids under 3D static mechanical stimulation. Mechanosensing of stiffness cues by these receptors regulates spheroid growth and the expression of markers involved in ion channel transport, ECM organization, and malignant phenotypes. Owing to the utility of a 3D culture system over traditional 2D systems in the study, this furthers our understanding of how OSCC progression is influenced by the stiffening of tumor tissues. Future work will involve the incorporation of other cell types crucial to the composition of the tumor microenvironment, such as immune cells, endothelial cells, and, especially, stromal cells that play a vital role in ECM organization and remodeling into our spheroid model and investigation of the effects of matrix stiffness mechanics therein. Our results also provide promise for future animal model studies to investigate the influence of the knockdown of specific mechanoreception genes on tumor growth *in vivo*. In the long term, this has untapped potential for adaption in systematic studies to develop therapies capable of intervening ECM stiffness-induced oncogenic signaling, cancer progression, and drug resistance.

METHODS

Fabrication of hydrogels

Matrigel matrix growth factor reduced (Corning, Corning, NY) and Matrigel matrix high concentration growth factor reduced (Corning, Corning, NY) were thawed overnight on ice prior to use. Matrigel matrix products were diluted to 3 and 12 mg/ml concentrations, defined as soft and stiff, respectively, using lot-specific protein concentrations in ice-cold PBS as per the manufacturer's instructions.

3D cell culture

Oral squamous cell carcinoma Cal27 cells (ATCC, Manassas, VA) were a kind gift from the Takiar-Wise Draper lab. Spheroids were generated in DMEM media (Corning, San Diego, CA) containing 10% fetal bovine serum (Fisher Scientific, Waltham, MA) that was superdepleted of extracellular vesicles via 18-hour ultracentrifugation at 100 000×g,[67] 1% penicillin-streptomycin (Fisher Scientific, Waltham, MA), 1% L-glutamine (Fisher Scientific, Waltham, MA), 1% sodium pyruvate (Fisher Scientific, Waltham, MA), and 1% non-essential amino acids (Fisher Scientific, Waltham, MA) using the media overlay technique.[68] Briefly, 24-well plates were coated with a thin layer of 3 or 12 mg/ml Matrigel and incubated for 30 min to allow the gel to solidify. Collected cells were counted upon trypsinization and suspended in media containing 1% Matrigel. This method enables cells to penetrate the underlying Matrigel coating and form spheroid aggregates. 10 000 cells in 500 μl suspension were plated on top of well coatings. Spheroids were cultured at 37 °C and 5% CO_2 with regular media changes.

Shear rheology

Relative stiffness measurements of hydrogels were performed by shear rheology as described previously.[69] Briefly, hydrogels (n = 3 per condition) were pipetted into 20 mm circular molds and solidified at 37 °C and 5% CO_2 for 30 min. Rheological characterization was performed using a Rheometer HR-20 (TA instruments, New Castle, DE) using a 20 mm parallel plate geometry. Solidified hydrogels were removed from the mold and carefully loaded onto the stepped lower geometry. The 20 mm upper geometry was lowered to just contact the top surface of the gel. Measurements were performed by applying

logarithmic strain sweeps from 0.1% to 100% strain at an angular frequency of 0.5 rad/s with five points collected per decade. Analysis was performed by extracting the storage modulus (G′) at 1% strain. The elastic modulus (E) was then determined from G′ using the following equation:

$$E = 2G'(1 + \upsilon), \quad (1)$$

where υ is the Poisson's ratio of 0.5 for hydrogels, E is the Elastic modulus, and G′ is the storage modulus.

Atomic force microscopy

Relative stiffness of hydrogels (n = 3 per condition) was also measured using a NanoWizard IV Atomic Force Microscope (AFM) (JPK Instruments, Berlin, Germany). Hydrogels were pipetted into 20 mm circular molds and solidified at 37 °C and 5% CO_2 for 30 min. The AFM head consisting of a CSC37 silicon nitride cantilever (k = 0.3–0.8 N/m, f = 20–40 kHz) (MikroMasch) was mounted on a M205 FA fluorescence stereo microscope (Leica, Werzlar, Germany) coupled with a JPK CellHesion module Z-axis piezo stage (JPK Instruments, Berlin, Germany), which allows indentation measurements up to a depth of ∼100 μm. Solidified gels were removed from the mold, and the sample slide was then placed onto the AFM stage to take AFM micrograph images in non-contact and Qi mode. Force–distance curves in a 10 × 10 μm square were measured for each sample under ambient conditions. Young's moduli of the hydrogels were determined by fitting the obtained force–distance curves with the modified Hertz model,[70] and resultant stiffness values were analyzed (n = 100 per sample).

Brightfield imaging

Brightfield imaging of spheroids was performed using a Nikon Eclipse TE2000-S microscope (Nikon, Melville, NY) equipped with an Andor NeoZyla 5.5 camera. Analysis was performed using ImageJ.

Confocal imaging

Day 14 spheroids were stained for immunofluorescence and imaged using confocal microscopy as described previously.[71] Briefly, spheroids were sequentially fixed in 3.7% formaldehyde, permeabilized in 0.5% TBSTX, and blocked using antibody dilution buffer (2% BSA in 0.1% TBSTX). All wash steps were performed in 0.1% TBSTX. Primary immunostaining was performed with 0.8 μg/ml APC anti-CD44 (Biolegend, San Diego, CA) and 2 μg/mL purified anti-Piezo1 (Biolegend, San Diego, CA) at 4 °C overnight. For secondary Piezo1 immunostaining, spheroids were stained with 2 μg/ml anti-rat AF594 secondary antibody (Biolegend, San Diego, CA) at room temperature for 3 h. The final pellet was washed, resuspended in PBS, and pipetted onto a glass slide. Once the spheroids had settled, Prolong Gold with DAPI (Invitrogen, Waltham, MA) was pipetted, and the suspension was covered using a coverslip. The edges of the slip were sealed with clear nail polish, and samples were stored at 4 °C until imaging. Confocal imaging was performed using a Nikon A1R inverted microscope (Nikon, Melville, NY) with multichannel z-stacks performed at 512-pixel resolution across the height of the spheroid. Representative maximum intensity projections and 3D alpha-blended projections were created using NIS Elements software.

Flow cytometry

Spheroids were harvested upon 14 days of culture using the cell recovery solution (Corning, Corning, NY). Harvested gels were held at 4 °C for 1 h and vortexed for complete disintegration of the Matrigel matrix as per the manufacturer's protocol. This non-enzymatic cell recovery solution-based method allows recovery from the Matrigel matrix without breaking up spheroids or impacting cellular viability.[72] The resulting suspension was centrifuged at 500xG and resuspended in TrypLE (Fisher Scientific, Waltham, MA) to lyse spheroids into single cells while maintaining cellular integrity.[73] For surface staining, cells were washed with staining buffer (5% FBS in PBS) and stained with 10 μg/ml APC anti-CD44 (Biolegend, San Diego, CA) surface marker or APC Mouse IgG1 Isotype control (Biolegend, San Diego, CA) for 20 min at 4 °C. Cells were then permeabilized and fixed using the Cytofix/Cytoperm Fixation/Permeabilization kit (BD Biosciences, Franklin Lakes, NJ), as per the manufacturer's instructions. For intracellular staining, unstained cells were permeabilized and fixed prior to staining with 25 μg/ml purified anti-Piezo1 (Biolegend, San Diego, CA) or AF594 Rat IgG2b Isotype control (Biolegend, San Diego, CA) for 20 min at 4 °C. Anti-piezo1 marked cells were washed twice and stained with 0.83 μg/ml anti-rat AF594 secondary (Biolegend, San Diego, CA) for 20 min at 4 °C. As a final step, all samples were washed and resuspended in staining buffer for flow cytometric analysis. Stained cells were analyzed with an Aurora flow cytometer (Cytek, Fremont, CA). Flow cytometry data were acquired for 30 000 events per sample and quantified as frequency using FlowJo software (FlowJo LLC, Ashland, OR) for three biological replicate experiments.

Histological staining and imaging

Day 14 spheroids were sectioned and stained for immunofluorescence imaging. Spheroids were sequentially fixed in 3.7% formaldehyde, permeabilized in 0.5% TBSTX, and pretreated with 30% sucrose. Embedded spheroids frozen in the OCT compound were sectioned at a thickness of 10 μm. Slides were pretreated using the Discovery XT automated platform (Ventana/Roche Tissue Diagnostics, Indianapolis, IN). Sections were stained with 10 μg/ml purified anti-Piezo1 (Biolegend, San Diego, CA) and 10 μg/ml anti-CD44 (Abcam, Cambridge, UK) at 4 °C overnight. Slides were rinsed with H_2O and the reaction buffer followed by secondary staining at a dilution of 1:100 for 1 h at room temperature. Stained slides were rinsed in H_2O, dried, and mounted with Vectashield Hard Mount with DAPI (H-1500). Confocal imaging was performed using a Nikon A1R inverted microscope (Nikon, Melville, NY) and processed using ImageJ.

RNA isolation and sequencing

Spheroids were harvested upon 14 days of culture using the cell recovery solution (Corning, Corning, NY). Harvested gels were held on ice and repeatedly vortex for complete disintegration of the Matrigel matrix. The resulting spheroid suspension was centrifuged and resuspended in RNAlater stabilization solution (Thermo Fisher, Waltham, MA). Total RNA was isolated using the mirVana miRNA Isolation kit (Thermo Fisher, Waltham, MA) from spheroid samples. Directional polyA RNA-seq was performed by the Genomics, Epigenomics, and Sequencing Core at the University of Cincinnati using established protocols as previously described[74,75] with updates. To summarize, the quality of total RNA was QC analyzed by

Bioanalyzer (Agilent, Santa Clara, CA). To enrich polyA RNA for library preparation, NEBNext Poly(A) mRNA Magnetic Isolation Module (New England BioLabs, Ipswich, MA) was used with 500 ng good quality total RNA as input. Next, the NEBNext Ultra II Directional RNA Library Prep kit (New England BioLabs, Ipswich, MA) was used for library preparation under PCR cycle number 10. After library QC and Qubit quantification (ThermoFisher, Waltham, MA), the normalized libraries were sequenced using NextSeq 2000 Sequencer (Illumina, San Diego, CA) under the setting of PE 2×61 bp to generate an average of 59.7M reads.

Bioinformatics analysis

RNA-seq reads in FASTQ format were first subjected to quality control to assess the need for trimming of adapter sequences or bad quality segments. The programs used in these steps were FastQC v0.11.7,[76] Trim Galore! v0.4.2,[77] and cutadapt v1.9.1.[78] The trimmed reads were aligned to the reference human genome version hg38 with the program STAR v2.6.1e.[79] Aligned reads were stripped of duplicate reads with the program sambamba v0.6.8.[80] Gene-level expression was assessed by counting features for each gene, as defined in the NCBI's RefSeq database.[81] Read counting was done with the program featureCounts v1.6.2 from the Rsubread package.[82] Raw counts were normalized as transcripts per million (TPM). Differential gene expressions between groups of samples were assessed with the R package DESeq2 v1.26.0.[83] Gene list and log2 fold change are used for GSEA analysis using GO pathway datasets. Plots were generated using the ggplot2[84] package and base graphics in R.

Statistical analysis

Data analysis was performed using GraphPad Prism 9 (GraphPad Software, La Jolla, CA). Quantitative data are expressed as mean ± SEM. All analyses involving two groups were evaluated using Student's t-test. RNA sequencing analysis plots including heatmaps were created using PlotsREasy (Bioinformatics Collaborative Services, CCHMC, Cincinnati, OH).

SUPPLEMENTARY MATERIAL

See the supplementary material for representative brightfield images of spheroids, RNA quality control data, and heatmap of all differentially expressed genes from RNA sequencing.

ACKNOWLEDGMENTS

The authors would like to thank Reinaldo Santos for rheometer training, Yara Izhiman and Maksym Krutko for assistance with sample handling, and Greg Macke for inputs on the preparation of figures. Rheology experiments were performed at the UC Advanced Materials Characterization Center (AMCC). This study was made possible, in part, using the Cincinnati Children's Bio-imaging and Analysis Facility (BAF; RRID: SCR_022628), Research Flow Cytometry Facility (RFCF; RRID: SCR_022635; supported by NIH Grant No. 1 P30 AR47363), Informatics Shared Facility (IS4R; RRID: SCR_022622), and Integrated Pathology Research Facility (IPRF; RRID: SCR_022637). RNA quality control and sequencing were performed by the UC Genomics, Epigenomics, and Sequencing Core (GESC; supported by CEG Grant NIEHS P30-ES006096 to Shuk-Mei Ho). We specifically acknowledge the assistance of Matt Kofron (BAF), Alyssa Sproles (RFCF), Xiang Zhang (GESC), Aditi Paranje (IS4R), Ashley Kuenzi (IS4R), and Betsy DiPasquale (IPRF).

This work was funded by the National Science Foundation NSF CAREER ECCS (No. 2046037) to Leyla Esfandiari.

Bulk RNA-sequencing data have been deposited with the Accession No. GSE262142.

AUTHOR DECLARATIONS

Conflict of Interest

The authors have no conflicts to disclose.

Ethics Approval

Ethics approval is not required.

Author Contributions

Maulee Sheth: Conceptualization (equal); Data curation (equal); Formal analysis (equal); Methodology (equal); Validation (equal); Visualization (equal); Writing – original draft (lead). **Manju Sharma:** Data curation (equal); Formal analysis (equal); Methodology (equal); Validation (equal); Visualization (equal). **Maria A. Lehn:** Methodology (equal); Writing – review & editing (equal). **HasanAl Reza:** Methodology (equal). **Takanori Takebe:** Resources (equal); Writing – review & editing (equal). **Vinita Takiar:** Writing – review & editing (equal). **Trisha Wise-Draper:** Methodology (equal); Resources (equal); Writing – review & editing (equal). **Leyla Esfandiari:** Conceptualization (lead); Funding acquisition (lead); Project administration (lead); Resources (lead); Supervision (lead); Writing – review & editing (lead).

DATA AVAILABILITY

The data that support the findings of this study are available within the article and its supplementary material.

REFERENCES

[1]K. A. Papavassiliou, E. K. Basdra, and A. G. Papavassiliou, "The emerging promise of tumour mechanobiology in cancer treatment," Eur. J Cancer **190**, 112938 (2023).
[2]L. Esfandiari, M. Paff, and W. C. Tang, "Initial studies of mechanical compression on neurogenesis with neonatal neural stem cells," Nanomedicine **8**(4), 415–418 (2012).
[3]B. Deng, Z. Zhao, W. Kong, C. Han, X. Shen, and C. Zhou, "Biological role of matrix stiffness in tumor growth and treatment," J. Transl. Med. **20**(1), 540 (2022).
[4]S. Ishihara and H. Haga, "Matrix stiffness contributes to cancer progression by regulating transcription factors," Cancers **14**(4), 1049 (2022).
[5]R. J. Pelham, Jr. and Y. Wang, "Cell locomotion and focal adhesions are regulated by substrate flexibility," Proc. Natl. Acad. Sci. U. S. A. **94**(25), 13661–13665 (1997).
[6]H. B. Wang, M. Dembo, and Y. L. Wang, "Substrate flexibility regulates growth and apoptosis of normal but not transformed cells," Am. J. Physiol. **279**(5), C1345–C1350 (2000).
[7]O. W. Petersen, L. Rønnov-Jessen, A. R. Howlett, and M. J. Bissell, "Interaction with basement membrane serves to rapidly distinguish growth and differentiation pattern of normal and malignant human breast epithelial cells," Proc. Natl. Acad. Sci. U. S. A. **89**(19), 9064–9068 (1992).
[8]Y. Li, N. Khuu, E. Prince, H. Tao, N. Zhang, Z. Chen, A. Gevorkian, A. P. McGuigan, and E. Kumacheva, "Matrix stiffness-regulated growth of breast tumor spheroids and their response to chemotherapy," Biomacromolecules **22**(2), 419–429 (2021).

[9]G. Cai, X. Li, S. S. Lin, S. J. Chen, N. C. Rodgers, K. M. Koning, D. Bi, and A. P. Liu, "Matrix confinement modulates 3D spheroid sorting and burst-like collective migration," bioRxiv (2024).
[10]N. Peela, F. S. Sam, W. Christenson, D. Truong, A. W. Watson, G. Mouneimne, R. Ros, and M. Nikkhah, "A three dimensional micropatterned tumor model for breast cancer cell migration studies," Biomaterials **81**, 72–83 (2016).
[11]S. C. Wei, L. Fattet, J. H. Tsai, Y. Guo, V. H. Pai, H. E. Majeski, A. C. Chen, R. L. Sah, S. S. Taylor, A. J. Engler *et al.*, "Matrix stiffness drives epithelial–mesenchymal transition and tumour metastasis through a TWIST1–G3BP2 mechanotransduction pathway," Nat. Cell Biol. **17**(5), 678–688 (2015).
[12]A. J. McKenzie, S. R. Hicks, K. V. Svec, H. Naughton, Z. L. Edmunds, and A. K. Howe, "The mechanical microenvironment regulates ovarian cancer cell morphology, migration, and spheroid disaggregation," Sci. Rep. **8**(1), 7228 (2018).
[13]M. Amereh, A. Seyfoori, B. Dallinger, M. Azimzadeh, E. Stefanek, and M. Akbari, "3D-printed tumor-on-a-chip model for investigating the effect of matrix stiffness on glioblastoma tumor invasion," Biomimetics **8**(5), 421 (2023).
[14]D. De Felice and A. Alaimo, "Mechanosensitive piezo channels in cancer: Focus on altered calcium signaling in cancer cells and in tumor progression," Cancers **12**(7), 1780 (2020).
[15]J. Wu, A. H. Lewis, and J. Grandl, "Touch, tension, and transduction—The function and regulation of piezo ion channels," Trends Biochem. Sci. **42**(1), 57–71 (2017).
[16]D. E. Clapham, "TRP channels as cellular sensors," Nature **426**(6966), 517–524 (2003).
[17]S. A. Mendoza, J. Fang, D. D. Gutterman, D. A. Wilcox, A. H. Bubolz, R. Li, M. Suzuki, and D. X. Zhang, "TRPV4-mediated endothelial Ca^{2+} influx and vasodilation in response to shear stress," Am. J. Physiol. **298**(2), H466–476 (2010).
[18]S. Sharma, R. Goswami, D. X. Zhang, and S. O. Rahaman, "TRPV4 regulates matrix stiffness and TGFβ1-induced epithelial-mesenchymal transition," J. Cell. Mol. Med. **23**(2), 761–774 (2019).
[19]Y. Jiang, H. Zhang, J. Wang, Y. Liu, T. Luo, and H. Hua, "Targeting extracellular matrix stiffness and mechanotransducers to improve cancer therapy," J. Hematol. Oncol. **15**(1), 34 (2022).
[20]K. Bera, A. Kiepas, Y. Zhang, S. X. Sun, and K. Konstantopoulos, "The interplay between physical cues and mechanosensitive ion channels in cancer metastasis," Front. Cell Dev. Biol. **10**, 954099 (2022).
[21]J. A. Dombroski, J. M. Hope, N. S. Sarna, and M. R. King, "Channeling the force: Piezo1 mechanotransduction in cancer metastasis," Cells **10**(11), 2815 (2021).
[22]S. V. Knoblauch, S. H. Desai, J. A. Dombroski, N. S. Sarna, J. M. Hope, and M. R. King, "Chemical activation and mechanical sensitization of Piezo1 enhance TRAIL-mediated apoptosis in glioblastoma cells," ACS Omega **8**(19), 16975–16986 (2023).
[23]B. Wang, W. Ke, K. Wang, G. Li, L. Ma, S. Lu, Q. Xiang, Z. Liao, R. Luo, Y. Song *et al.*, "Mechanosensitive ion channel Piezo1 activated by matrix stiffness regulates oxidative stress-induced senescence and apoptosis in human intervertebral disc degeneration," Oxid Med. Cell. Longevity **2021**, 8884922.
[24]Y. Wu, X. Xu, F. Liu, Z. Jing, D. Shen, P. He, T. Chen, T. Wu, H. Jia, D. Mo *et al.*, "Three-dimensional matrix stiffness activates the PIEZO1-AMPK-autophagy axis to regulate the cellular osteogenic differentiation," ACS Biomater. Sci. Eng. **9**(8), 4735–4746 (2023).
[25]A. Barsouk, J. S. Aluru, P. Rawla, K. Saginala, and A. Barsouk, "Epidemiology, risk factors, and prevention of head and neck squamous cell carcinoma," Med. Sci. **11**(2), 42 (2023).
[26]K. Pogoda, M. Ciesluk, P. Deptula, G. Tokajuk, E. Piktel, G. Krol, J. Reszec, and R. Bucki, "Inhomogeneity of stiffness and density of the extracellular matrix within the leukoplakia of human oral mucosa as potential physicochemical factors leading to carcinogenesis," Transl. Oncol. **14**(7), 101105 (2021).
[27]L. Jingyuan, L. Yu, J. Hong, W. Tao, L. Kan, L. Xiaomei, L. Guiqing, and L. Yujie, "Matrix stiffness induces an invasive-dormant subpopulation via cGAS-STING axis in oral cancer," Transl. Oncol. **33**, 101681 (2023).
[28]B. F. Matte, A. Kumar, J. K. Placone, V. G. Zanella, M. D. Martins, A. J. Engler, and M. L. Lamers, "Matrix stiffness mechanically conditions EMT and migratory behavior of oral squamous cell carcinoma," J. Cell Sci. **132**(1), jcs224360 (2019).
[29]D. Lee, H. Zhang, and S. Ryu, "Elastic modulus measurement of hydrogels," in *Cellulose-Based Superabsorbent Hydrogels*, edited by M. I. H. Mondal (Springer International Publishing, 2018), pp 1–21.
[30]A. Otero-Sobrino, P. Blanco-Carlón, M. A. Navarro-Aguadero, M. Gallardo, J. Martínez-López, and M. Velasco-Estévez, "Mechanosensitive ion channels: Their physiological importance and potential key role in cancer," Int. J. Mol. Sci. **24**(18), 13710 (2023).
[31]Y. Zhou, C. Zhang, Z. Zhou, C. Zhang, and J. Wang, "Identification of key genes and pathways associated with *PIEZO1* in bone-related disease based on bioinformatics," Int. J. Mol. Sci. **23**(9), 5250 (2022).
[32]P. Besson, V. Driffort, E. Bon, F. Gradek, S. Chevalier, and S. Roger, "How do voltage-gated sodium channels enhance migration and invasiveness in cancer cells?," Biochim. Biophys. Acta, Biomembr. **1848**(10 Pt B), 2493–2501 (2015).
[33]S. Iacobas, B. Amuzescu, and D. A. Iacobas, "Transcriptomic uniqueness and commonality of the ion channels and transporters in the four heart chambers," Sci. Rep. **11**(1), 2743 (2021).
[34]Y. R. Cheng, B. Y. Jiang, and C. C. Chen, "Acid-sensing ion channels: Dual function proteins for chemo-sensing and mechano-sensing," J. Biomed. Sci. **25**(1), 46 (2018).
[35]M. Shekarabi, J. Zhang, A. R. Khanna, D. H. Ellison, E. Delpire, and K. T. Kahle, "WNK kinase signaling in ion homeostasis and human disease," Cell Metab. **25**(2), 285–299 (2017).
[36]A. Biasiotta, D. D'Arcangelo, F. Passarelli, E. M. Nicodemi, and A. Facchiano, "Ion channels expression and function are strongly modified in solid tumors and vascular malformations," J. Transl. Med. **14**(1), 285 (2016).
[37]B. K. Puri, "Calcium signaling and gene expression," in *Calcium Signaling*, edited by M. S. Islam (Springer International Publishing, 2020), pp. 537–545.
[38]P. Buttner, L. Ueberham, M. B. Shoemaker, D. M. Roden, B. Dinov, G. Hindricks, A. Bollmann, and D. Husser, "Identification of central regulators of calcium signaling and ECM-receptor interaction genetically associated with the progression and recurrence of atrial fibrillation," Front. Genet. **9**, 162 (2018).
[39]Q. Zhong, Q. Zhong, X. Cai, and R. Wu, "Identification and validation of an ECM organization-related gene signature as a prognostic biomarker and therapeutic target for glioma patients," Genes Genomics **45**(9), 1211–1226 (2023).
[40]J. Winkler, A. Abisoye-Ogunniyan, K. J. Metcalf, and Z. Werb, "Concepts of extracellular matrix remodelling in tumour progression and metastasis," Nat. Commun. **11**(1), 5120 (2020).
[41]Q. Xiao and G. Ge, "Lysyl oxidase, extracellular matrix remodeling and cancer metastasis," Cancer Microenviron. **5**(3), 261–273 (2012).
[42]R. Moreno-Vicente, D. M. Pavon, I. Martin-Padura, M. Catala-Montoro, A. Diez-Sanchez, A. Quilez-Alvarez, J. A. Lopez, M. Sanchez-Alvarez, J. Vazquez, R. Strippoli *et al.*, "Caveolin-1 modulates mechanotransduction responses to substrate stiffness through actin-dependent control of YAP," Cell Rep. **25**(6), 1622–1635 (2018).
[43]S. D. Li, M. Ma, H. Li, A. Waluszko, T. Sidorenko, E. E. Schadt, D. Y. Zhang, R. Chen, and F. Ye, "Cancer gene profiling in non-small cell lung cancers reveals activating mutations in JAK2 and JAK3 with therapeutic implications," Genome Med. **9**(1), 89 (2017).
[44]E. Crosas-Molist, R. Samain, L. Kohlhammer, J. L. Orgaz, S. L. George, O. Maiques, J. Barcelo, and V. Sanz-Moreno, "Rho GTPase signaling in cancer progression and dissemination," Physiol. Rev. **102**(1), 455–510 (2022).
[45]W. Dai, Y. Xiao, W. Tang, J. Li, L. Hong, J. Zhang, M. Pei, J. Lin, S. Liu, X. Wu *et al.*, "Identification of an EMT-related gene signature for predicting overall survival in gastric cancer," Front. Genet. **12**, 661306 (2021).
[46]L. Wu, S. Amjad, H. Yun, S. Mani, and M. de Perrot, "A panel of emerging EMT genes identified in malignant mesothelioma," Sci. Rep. **12**(1), 1007 (2022).
[47]S. Usman, A. Jamal, M. T. Teh, and A. Waseem, "Major molecular signaling pathways in oral cancer associated with therapeutic resistance," Front. Oral Health **1**, 603160 (2020).
[48]S. H. D. Wong, B. Yin, Z. Li, W. Yuan, Q. Zhang, X. Xie, Y. Tan, N. Wong, K. Zhang, and L. Bian, "Mechanical manipulation of cancer cell tumorigenicity via heat shock protein signaling," Sci. Adv. **9**(27), eadg9593 (2023).
[49]O. Habanjar, M. Diab-Assaf, F. Caldefie-Chezet, and L. Delort, "3D cell culture systems: Tumor application, advantages, and disadvantages," Int. J. Mol. Sci. **22**(22), 22 (2021).
[50]L. Tomasetti, R. Liebl, D. S. Wastl, and M. Breunig, "Influence of PEGylation on nanoparticle mobility in different models of the extracellular matrix," Eur. J. Pharm. Biopharm. **108**, 145–155 (2016).

[51]C. S. Hughes, L. M. Postovit, and G. A. Lajoie, "Matrigel: A complex protein mixture required for optimal growth of cell culture," Proteomics **10**(9), 1886–1890 (2010).
[52]Y. Li and E. Kumacheva, "Hydrogel microenvironments for cancer spheroid growth and drug screening," Sci. Adv. **4**(4), eaas8998 (2018).
[53]F. Arends, C. Nowald, K. Pflieger, K. Boettcher, S. Zahler, and O. Lieleg, "The biophysical properties of basal lamina gels depend on the biochemical composition of the gel," PLoS One **10**(2), e0118090 (2015).
[54]M. H. Zaman, L. M. Trapani, A. L. Sieminski, D. MacKellar, H. Gong, R. D. Kamm, A. Wells, D. A. Lauffenburger, and P. Matsudaira, "Migration of tumor cells in 3D matrices is governed by matrix stiffness along with cell-matrix adhesion and proteolysis," Proc. Natl. Acad. Sci. U. S. A. **103**(29), 10889–10894 (2006).
[55]S. S. Soofi, J. A. Last, S. J. Liliensiek, P. F. Nealey, and C. J. Murphy, "The elastic modulus of Matrigel™ as determined by atomic force microscopy," J. Struct. Biol. **167**(3), 216–219 (2009).
[56]M. Cavo, M. Fato, L. Penuela, F. Beltrame, R. Raiteri, and S. Scaglione, "Microenvironment complexity and matrix stiffness regulate breast cancer cell activity in a 3D in vitro model," Sci. Rep. **6**, 35367 (2016).
[57]M. Kalli and T. Stylianopoulos, "Defining the role of solid stress and matrix stiffness in cancer cell proliferation and metastasis," Front. Oncol. **8**, 55 (2018).
[58]X. Li and J. Wang, "Mechanical tumor microenvironment and transduction: Cytoskeleton mediates cancer cell invasion and metastasis," Int. J. Biol. Sci. **16**(12), 2014–2028 (2020).
[59]X. Chen, S. Wanggou, A. Bodalia, M. Zhu, W. Dong, J. J. Fan, W. C. Yin, H. K. Min, M. Hu, D. Draghici *et al.*, "A feedforward mechanism mediated by mechanosensitive ion channel PIEZO1 and tissue mechanics promotes glioma aggression," Neuron **100**(4), 799–815 (2018).
[60]A. Koussounadis, S. P. Langdon, I. H. Um, D. J. Harrison, and V. A. Smith, "Relationship between differentially expressed mRNA and mRNA-protein correlations in a xenograft model system," Sci. Rep. **5**, 10775 (2015).
[61]Y. Liu, A. Beyer, and R. Aebersold, "On the dependency of cellular protein levels on mRNA abundance," Cell **165**(3), 535–550 (2016).
[62]S. Göransson, S. Chen, H. Olofsson, O. Larsson, and S. Strömblad, "An extracellular matrix stiffness-induced breast cancer cell transcriptome resembles the transition from ductal carcinoma in situ (DCIS) to invasive ductal carcinoma (IDC)," Biochem. Biophys. Res. Commun. **654**, 73–79 (2023).
[63]M. Sheth and L. Esfandiari, "Bioelectric dysregulation in cancer initiation, promotion, and progression," Front. Oncol. **12**, 846917 (2022).
[64]B. B. Silver, S. X. Zhang, E. M. Rabie, and C. M. Nelson, "Substratum stiffness tunes membrane voltage in mammary epithelial cells," J. Cell Sci. **134**(13), jcs256313 (2021).
[65]B. B. Silver and C. M. Nelson, "The bioelectric code: Reprogramming cancer and aging from the interface of mechanical and chemical microenvironments," Front. Cell Dev. Biol. **6**, 21 (2018).
[66]C. Huang, C. Yoon, X. H. Zhou, Y. C. Zhou, W. W. Zhou, H. Liu, X. Yang, J. Lu, S. Y. Lee, and K. Huang, "ERK1/2-Nanog signaling pathway enhances CD44(+) cancer stem-like cell phenotypes and epithelial-to-mesenchymal transition in head and neck squamous cell carcinomas," Cell Death Dis. **11**(4), 266 (2020).
[67]S. Langevin, D. Kuhnell, T. Parry, J. Biesiada, S. Huang, T. Wise-Draper, K. Casper, X. Zhang, M. Medvedovic, and S. Kasper, "Comprehensive microRNA-sequencing of exosomes derived from head and neck carcinoma cells *in vitro* reveals common secretion profiles and potential utility as salivary biomarkers," Oncotarget **8**(47), 82459–82474 (2017).
[68]C. Jubelin, J. Muñoz-Garcia, D. Cochonneau, E. Ollivier, F. Vallette, M. F. Heymann, L. Oliver, and D. Heymann, "Technical report: Liquid overlay technique allows the generation of homogeneous osteosarcoma, glioblastoma, lung and prostate adenocarcinoma spheroids that can be used for drug cytotoxicity measurements," Front. Bioeng. Biotechnol. **11**, 1260049 (2023).
[69]T. R. Cox and C. D. Madsen, "Relative stiffness measurements of cell-embedded hydrogels by shear rheology *in vitro*," Bio-Protoc. **7**(1), e2101 (2017).
[70]I. N. Sneddon, "The relation between load and penetration in the axisymmetric Boussinesq problem for a punch of arbitrary profile," Int. J. Eng. Sci. **3**(1), 47–57 (1965).
[71]K. N. Bergdorf, C. J. Phifer, M. E. Bechard, M. A. Lee, O. G. McDonald, E. Lee, and V. L. Weiss, "Immunofluorescent staining of cancer spheroids and fine-needle aspiration-derived organoids," STAR Protoc. **2**(2), 100578 (2021).
[72]M. Wang, H. Yu, T. Zhang, L. Cao, Y. Du, Y. Xie, J. Ji, and J. Wu, "In-depth comparison of Matrigel dissolving methods on proteomic profiling of organoids," Mol. Cell. Proteomics **21**(1), 100181 (2022).
[73]T. Miwa, A. Idiris, and H. Kumagai, "High-throughput 3D spheroid formation and effective cardiomyocyte differentiation from human iPS cells using the microfabric vessels EZSPHERE™," Bio-Protoc. **11**(21), e4203 (2021).
[74]K. Qiu, W. Zou, Z. Fang, Y. Wang, S. Bell, X. Zhang, Z. Tian, X. Xu, B. Ji, D. Li *et al.*, "2D MoS_2 and BN nanosheets damage mitochondria through membrane penetration," ACS Nano **17**(5), 4716–4728 (2023).
[75]Z. Wei, P. Gordon, C. Hao, J. Huangfu, E. Fan, X. Zhang, H. Yan, and X. Fan, "Aged lens epithelial cells suppress proliferation and epithelial-mesenchymal transition-relevance for posterior capsule opacification," Cells **11**(13), 2001 (2022).
[76]See http://www.bioinformatics.babraham.ac.uk/projects/fastqc for "FastQC: A Quality Control Tool for High Throughput Sequence Data" (accessed August 2, 2024).
[77]See https://www.bioinformatics.babraham.ac.uk/projects/trim_galore for "A Wrapper Tool Around Cutadapt and FastQC to Consistently Apply Quality and Adapter Trimming to FastQ Files, With Some Extra Functionality for MspI-Digested RRBS-Type (Reduced Representation Bisufite-Seq) Libraries" (accessed August 2, 2024).
[78]M. Martin, "Cutadapt removes adapter sequences from high-throughput sequencing reads," EMBnet. J. **17**(1), 3 (2011).
[79]A. Dobin, C. A. Davis, F. Schlesinger, J. Drenkow, C. Zaleski, S. Jha, P. Batut, M. Chaisson, and T. R. Gingeras, "STAR: Ultrafast universal RNA-seq aligner," Bioinformatics **29**(1), 15–21 (2012).
[80]A. Tarasov, A. J. Vilella, E. Cuppen, I. J. Nijman, and P. Prins, "Sambamba: Fast processing of NGS alignment formats," Bioinformatics **31**(12), 2032–2034 (2015).
[81]N. A. O'Leary, M. W. Wright, J. R. Brister, S. Ciufo, D. Haddad, R. McVeigh, B. Rajput, B. Robbertse, B. Smith-White, D. Ako-Adjei *et al.*, "Reference sequence (RefSeq) database at NCBI: Current status, taxonomic expansion, and functional annotation," Nucl. Acids Res. **44**(D1), D733–D745 (2015).
[82]Y. Liao, G. K. Smyth, and W. Shi, "The R package *Rsubread* is easier, faster, cheaper and better for alignment and quantification of RNA sequencing reads," Nucl. Acids Res. **47**(8), e47 (2019).
[83]M. I. Love, W. Huber, and S. Anders, "Moderated estimation of fold change and dispersion for RNA-seq data with DESeq2," Genome Biol. **15**(12), 550 (2014).
[84]H. Wickham, *ggplot2: Elegant Graphics for Data Analysis* (Springer-Verlag, New York, 2016).